PHYSICAL REVIEW B **81**, 041203(R) (2010)

Skyrmion lattice in the doped semiconductor $Fe_{1-x}Co_xSi$

W. Münzer,[1] A. Neubauer,[1] T. Adams,[1] S. Mühlbauer,[1] C. Franz,[1] F. Jonietz,[1] R. Georgii,[2,1] P. Böni,[1] B. Pedersen,[2] M. Schmidt,[3] A. Rosch,[4] and C. Pfleiderer[1,*]

[1]*Physik Department E21, Technische Universität München, D-85748 Garching, Germany*

[2]*Forschungsneutronenquelle Heinz-Maier-Leibnitz (FRM II), Technische Universität München, D-85748 Garching, Germany*

[3]*MPI für Chemische Physik fester Stoffe, Nöthnitzer Straße 40, D-01187 Dresden, Germany*

[4]*Institut für Theoretische Physik, Universität zu Köln, Zülpicher Str. 77, D-50937 Cologne, Germany*

(Received 14 November 2009; published 20 January 2010)

We report a comprehensive small angle neutron scattering study of the magnetic phase diagram of the doped semiconductor $Fe_{1-x}Co_xSi$ for $x=0.2$. For magnetic field parallel to the neutron beam we observe a sixfold intensity pattern under field cooling. The regime of the skyrmion lattice is highly hysteretic and extents over a wide temperature range as may be expected due to the site disorder of the Fe and Co atoms. Our study identifies $Fe_{1-x}Co_xSi$ as the second material in which a skyrmion lattice forms and establishes that skyrmion lattices exist also in doped semiconductors.

DOI: 10.1103/PhysRevB.81.041203 PACS number(s): 72.80.Ga, 75.25.−j, 75.20.Ck, 75.30.−m

Recently we identified the formation of a lattice of skyrmion lines, a type of vortices, in the cubic transition metal compound MnSi.[1,2] The skyrmion lattice may be viewed as a crystallization of topologically stable particlelike knots of the spin structure that is driven by thermal fluctuations. It decouples very efficiently from the atomic lattice and is always strictly perpendicular to the applied field. As a new form of magnetic order that was long anticipated to exist in anisotropic materials,[3] the skyrmion lattice in MnSi attracts interdisciplinary interest as an analog of similar lattice structures in nuclear physics,[4,5] quantum Hall systems,[6,7] and liquid crystals.[8] All of these aspects make it of central importance to establish whether the skyrmion lattice in MnSi is just a material specific peculiarity or if it is the first example of a more general phenomenon. The latter is suggested by the theoretical treatment in Ref. 1. To settle this issue requires evidence of skyrmion lattices and related spin structures in further magnetic materials, preferably with different electronic properties. For instance, because MnSi is a pure metal key questions concern if skyrmion lattices are sensitive to disorder and whether they also exist in semiconductors and insulators.

The series of isostructural B20 transition metal silicides TSi (T=Fe,Co,Mn) is ideally suited to study whether skyrmion lattices occur generically in magnets without inversion symmetry because the electronic properties of TSi compounds vary substantially. In contrast to MnSi the system FeSi is a nonmagnetic insulator with strong electronic correlations[9] while its sibling CoSi is a diamagnetic metal.[10] For increasing Co content the series $Fe_{1-x}Co_xSi$ displays an insulator to metal transition at $x=0.02$ with a dome of helimagnetic order in the range $0.05 \leq x \leq 0.7$.[11] The magnetotransport in $Fe_{1-x}Co_xSi$ attracts interest in its own right.[12,13]

The helimagnetic order in $Fe_{1-x}Co_xSi$ results from a hierarchy of energy scales, starting with ferromagnetic exchange on the strongest scale favoring parallel spin alignment and Dzyaloshinsky-Moriya (DM) spin-orbit interactions, permitted in the noncentrosymmetric B20 structure, favoring perpendicular spin alignment on a weaker scale. With increasing x the wavelength of the resulting helical modulation varies from about 200 to 2000 Å.[11,14–16] The propagation direction of the helical modulation is determined by crystal-field interactions on the weakest scale. Based on small angle neutron scattering study (SANS) experiments[15,17,18] and Lorentz force microscopy[19] it was concluded that the propagation axis of the helix in $Fe_{1-x}Co_xSi$ is $\langle 100 \rangle$ for all x. While this differs distinctly from the propagation direction in MnSi, where it is $\langle 111 \rangle$, it is perfectly consistent with the B20 cubic crystal structure.[20,21] Further, while the DM interaction and the crystal structure have the same chirality in MnSi,[22] they have opposite chirality in $Fe_{1-x}Co_xSi$.[16] Finally, due to the doping in $Fe_{1-x}Co_xSi$ there must be strong site disorder of the Fe and Co atoms even in excellent single crystals. Thus, although $Fe_{1-x}Co_xSi$ and MnSi exhibit rather similar magnetic properties, there are strong differences of the underlying electronic structure, making $Fe_{1-x}Co_xSi$ an ideal system to test the general nature of skyrmion lattices.

The magnetic phase diagram of $Fe_{1-x}Co_xSi$ exhibits three prominent features.[15,17,18] First, a state with a helimagnetic modulation up to a critical field B_{c1} in the following is referred to as zero-field cooled state. Second, for a magnetic field in the range $B_{c1} < B < B_{c2}$ a helical modulation parallel to the magnetic field is stabilized, forming the so-called conical state. Third, in the so-called A phase, a small pocket just below T_c, the helical modulation is perpendicular to the applied magnetic field. Prior to the work reported here all studies were carried out with the field perpendicular to the neutron beam. Because this configuration is mostly sensitive to helical components parallel to the field and only selected helical components perpendicular to the field, the information on the A phase was incomplete and it was believed that the A phase represents a single-Q helical state.[15,17,18]

In the following we report a comprehensive SANS study of the magnetic phase diagram of $Fe_{1-x}Co_xSi$ for $x=0.2$ and $x=0.25$. In contrast to previous SANS studies[15,17,18] we explore the magnetic phase diagram also with the magnetic field *parallel* to the incident neutron beam. This configuration is sensitive to *all* helical modulations perpendicular to the field. We also determined differences of the phase diagram for zero-field cooling (ZFC) and field cooling (FC). As

our main result we identify the A phase of $Fe_{1-x}Co_xSi$ as a hexagonal skyrmion lattice akin that seen in MnSi. As opposed to MnSi, the skyrmion lattice yields strong hysteretic features and may be observed over a large temperature range. Thus we identify a second example of a skyrmion lattice, however, in a doped semiconductor with strong disorder (the latter is inferred from the nonstoichiometric composition and the absence of a superstructure as reported below). In addition we find that the ZFC state, long known to be metastable,[17] is characterized by scattering intensity on the surface of a small sphere in reciprocal space with broad maxima in the ⟨110⟩ direction. This is strongly reminiscent of the partial magnetic order in MnSi at high pressure.[23]

For our study several single crystals were grown at TUM by optical float zoning with a UHV-compatible image furnace. Laue x-ray diffraction, energy dispersive x-rays (EDX), polarized light microscopy, and single-crystal neutron diffraction established an excellent sample quality. The magnetotransport properties, magnetization, and specific heat were in excellent agreement with the literature.[13] All samples were oriented using Laue x-ray diffraction. A large single crystal with $x=0.2$, studied most extensively, was additionally oriented on the diffractometer RESI at FRM II. Using neutrons with a wavelength $\lambda=1.0402$ Å $\pm 1\%$ we determined ten Bragg peaks that were fitted simultaneously. The sample had a lattice constant $a=4.483\pm0.02$ Å with an excellent resolution-limited mosaic spread better than 0.2°. We further confirmed within the resolution limit that there were no superstructures, structural short-range order, or lattice distortions. The modulus of the helical modulation $Q \approx 0.017$ Å^{-1}, transition temperature $T_c \approx 30$ K, and the lattice constant were in excellent agreement with Refs. 17, 18, and 24 but differed from crystals grown in a triarc furnace.[15]

Our SANS studies were carried out at the diffractometer MIRA at FRM II using neutrons with a wavelength $\lambda=9.7$ Å $\pm 5\%$. Backgrounds were determined at high temperatures and subtracted accordingly. A Cd marker on the sample support confirmed that the sample was always oriented correctly. The sample was cooled with a pulse-tube cooler. Magnetic fields up to 0.3 T were applied with a bespoke set of Helmholtz coils. Data were recorded for a fixed sample orientation following rocking scans with respect to a vertical axis of typically ±15°.

In the following we focus on the ZFC state and the A phase. Figures 1(A)–1(C) show the scattering patterns of the ZFC state for $x=0.2$ for three different directions, namely, the crystallographic ⟨111⟩, ⟨110⟩, and ⟨100⟩ axes, respectively. In this order of orientation the scattering patterns are characterized by a uniform ring, a ring with minima for ⟨100⟩ (horizontal direction), and a ring with minima for both ⟨100⟩ directions (the diagonals), respectively. Taken together Figs. 1(A)–1(C), we establish that the ZFC state is characterized by intensity on the surface of a small sphere in reciprocal space with broad intensity maxima for ⟨110⟩.[25]

This contrasts previous studies, where a ZFC intensity distribution was reported with broad maxima for ⟨100⟩.[15,17,18] We have therefore confirmed our results for several samples with $x=0.2$ from different growths. Moreover, for $x=0.25$ we find a similar scattering distribution in the ZFC state, i.e., maxima for ⟨110⟩ (data not shown[26]). Thus data in Refs. 15 and 18 may have accidentally been indexed incorrectly or a sample dependence exists, e.g., due to the different methods of growth, where our samples seem excellent (see above). The broad intensity maxima for ⟨110⟩ in the ZFC state are also unusual because the propagation direction of the helical modulation in the cubic B20 crystal structure in leading order may be either parallel to ⟨111⟩ or ⟨100⟩.[20,21] In fact, the ZFC intensity distribution corresponds to the partially ordered state of MnSi.[23]

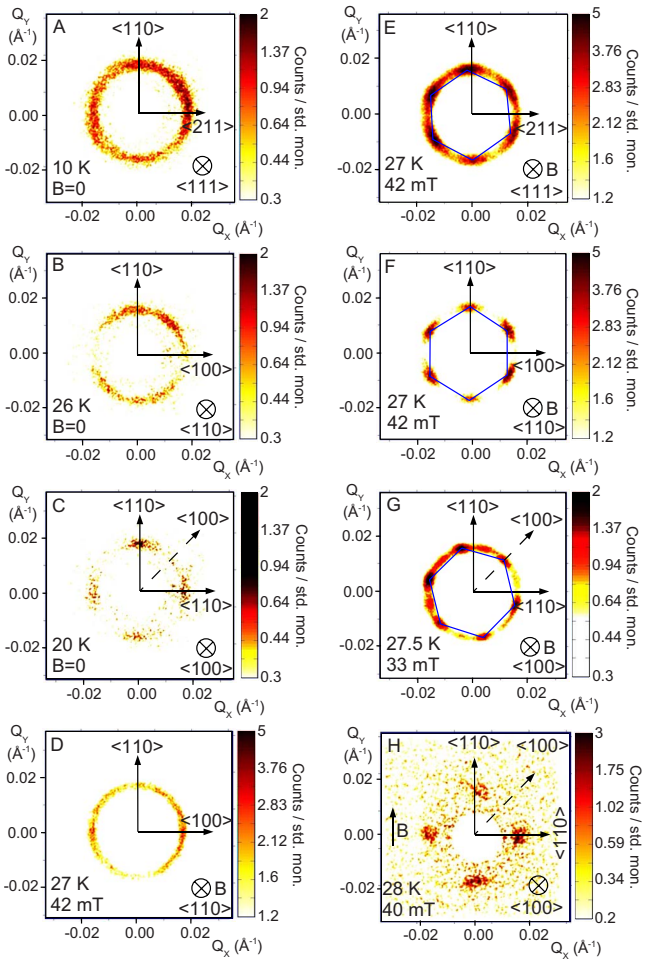

FIG. 1. (Color online) Typical SANS data of $Fe_{1-x}Co_xSi$ for $x=0.2$. (A)–(C) Intensity after ZFC. (D) A phase after ZFC for increasing B parallel to the neutron beam. (E)–(G) Sixfold intensity distribution in the A phase after field cooling for B parallel to the neutron beam. (H) A phase after field cooling for B perpendicular to the neutron beam.

Shown in Figs. 1(D)–1(G) are typical intensity patterns in the A phase. These patterns are exclusively seen in the plane perpendicular to the magnetic field. After ZFC and for increasing field we observe a uniform ring of intensity regardless of the crystallographic orientation [Fig. 1(D)]. In contrast, the intensity pattern after FC in the A phase is characterized by a sixfold symmetry. For the ⟨111⟩ and ⟨110⟩ directions six spots are observed as shown in Figs. 1(E) and 1(F), respectively, where two of the spots are aligned with a ⟨110⟩ axis. For the ⟨100⟩ direction the intensity pattern in the A phase is composed of 12 spots comprising two sets of six spots of differing intensity [Fig. 1(G)]. Each set of six spots

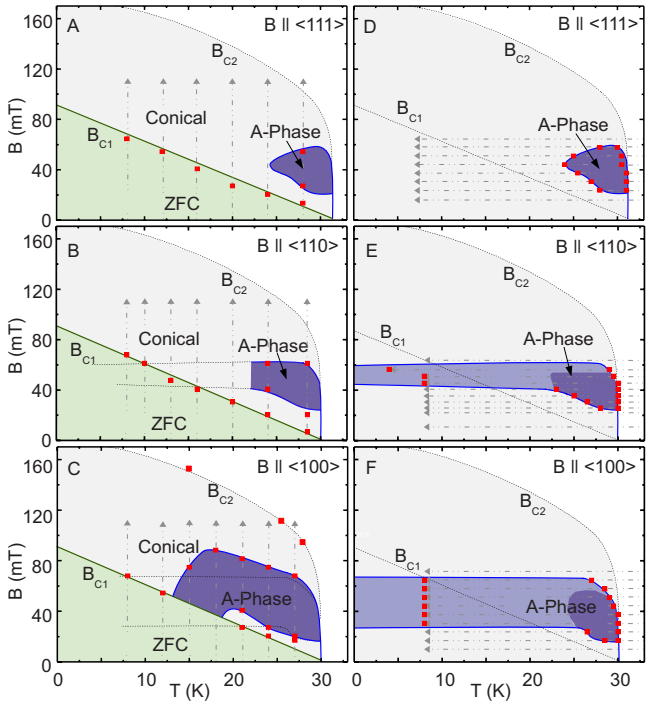

FIG. 2. (Color online) Magnetic phase diagram of $Fe_{1-x}Co_xSi$ for $x=0.2$. Gray arrows show the location of temperature and field scans. Red/Gray data points show transition fields and temperatures as determined in these scans. Panels (A)–(C) show the magnetic phase diagrams after ZFC; in the green shaded area the scattering intensity of the ZFC state is observed. Panels (D)–(F) show the magnetic phase diagrams for FC. Across the dark blue/gray area the intensity displays a maximum.

is aligned with one of the two ⟨100⟩ directions in this plane. This is a characteristic of two domain populations (similar effects have been seen in superconducting flux line lattices, e.g., as described in Ref. 27). We have finally also confirmed the formation of the conical phase, which coexists with the A phase in Fig. 1(H) (horizontal and vertical spots are due to the A phase and conical phase, respectively).

Shown in Fig. 2 is the magnetic phase diagram for $x=0.2$ (similar diagrams for $x=0.25$ are not shown). We find excellent agreement with published work where data are available. Starting from a ZFC state we observe (i) scattering intensity with broad maxima for ⟨110⟩ up to B_{c1}, where $B_{c1}(T\rightarrow 0)\approx 95$ mT and $dB_{c1}/dT\approx -3$ mT K^{-1} are isotropic (green shading), (ii) a conical phase as reported before (gray shading), and (iii) a ring of intensity in the A phase, where the wave vector is perpendicular to the field (blue shading). For FC the salient features are the following: (i) the ZFC scattering intensity is never observed, (ii) scattering intensity in the A phase with a sixfold symmetry and wave vectors perpendicular to the field (blue shading), and (iii) a small field range in which the A phase exists down to the lowest temperatures (this is not seen for field in the ⟨111⟩ direction). The regime where the intensity in the A phase displays a maximum is shown as dark blue shading, while the remaining regime is shown in light blue shading.

The integrated intensity shown in Fig. 3 allows us to illustrate metastable aspects of the ZFC state and the A phase.

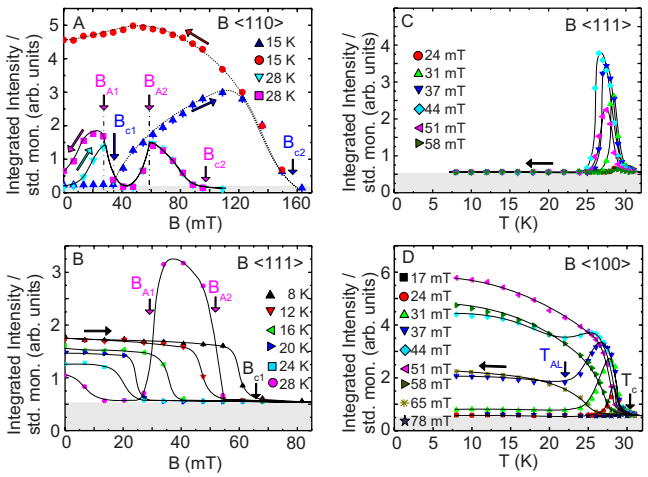

FIG. 3. (Color online) Temperature and magnetic field dependences of the integrated scattering intensity. (A) Intensity for $B\|\langle 110\rangle$ and B perpendicular to the neutron beam. (B) Intensity for $B\|\langle 111\rangle$ and B parallel to the neutron beam. (C) and (D) Intensity for B parallel to neutron beam under FC. All panels use the same arbitrary scale; gray shading shows the background.

For *B perpendicular* to the neutron beam we reproduced published results.[15] As shown in Fig. 3(A) for ⟨110⟩, there is essentially no intensity up to B_{c1} for increasing B and low T above which the conical phase appears. In contrast, for decreasing field the intensity remains unchanged high below B_{c1}. In the vicinity of T_c the intensity displays a reversible minimum in the A phase between B_{A1} and B_{A2}, where the intensity includes contributions of the A phase and the conical phase [see Fig. 1(H)].

Scans for field parallel to the neutron beam shown in Figs. 3(B)–3(D) are the counterpart to that shown in Fig. 3(A), notably they show all helical components perpendicular to the field. For ⟨111⟩ and increasing field the ZFC intensity well below T_c is unchanged until it vanishes above B_{c1} [Fig. 3(B)]. However, in field scans of decreasing strength the ZFC intensity is not recovered (data not shown). Near T_c the intensity reversibly shows a maximum in the A phase (data at 28 K). In temperature scans a corresponding maximum is seen in the A phase [see Fig. 3(C) for ⟨111⟩]. An additional feature emerges in temperature scans for ⟨100⟩ and ⟨110⟩, shown in Fig. 3(D) for ⟨100⟩. For $B>31$ mT and FC the intensity displays not only a maximum but also an additional increase down to the lowest temperatures. The regime of the maximum near T_c agrees between ZFC and FC for all three directions (compare dark blue shading in Figs. 2(A)–2(C) with Figs. 2(D)–2(F), respectively). Interestingly, for ⟨100⟩ the A phase even borders on the ZFC state [Fig. 2(C)].

The scattering pattern and hysteretic behavior reported here are fully consistent with a scenario where the A phase is thermodynamically stable in the dark blue areas and metastable in the light blue region. The characterizing sixfold pattern is, however, directly observable only for FC. Due to the disorder and the extremely weak anisotropy,[1] the spin structure is not able to lock to the underlying crystalline structure for ZFC so that only rings of intensity can be observed as shown in Fig. 1(D).

The outstanding experimental characteristic of the scatter-

ing pattern in the A phase is the sixfold symmetry and that it aligns strictly perpendicular to the applied magnetic field. The observation of two domain populations for field parallel $\langle 100 \rangle$ establishes that this stable sixfold symmetry, independent of its orientation, is impossible to explain with a multidomain helical order and has to originate in a crystal-like magnetic structure. Also, the controlled theoretical framework presented in Ref. 1 readily explains the sixfold pattern including its orientation as a skyrmion lattice. Moreover, it also predicts the magnetic phase diagram, notably the small phase pocket below T_c. There is hence no doubt that the A phase in $Fe_{1-x}Co_xSi$ represents a skyrmion lattice.

The trend to align two intensity maxima along $\langle 110 \rangle$ for field in the $\langle 111 \rangle$ and $\langle 110 \rangle$ directions can be easily explained in the model described in Ref. 1 by adding, e.g., an anisotropy term $\Sigma_{\vec{k}}(k_x^6+k_y^6+k_z^6)\vec{m}_{\vec{k}}\vec{m}_{-k}$ with a positive coefficient. By symmetry, this term to linear order does not cause any alignment of the orientation of the skyrmion lattice for field parallel $\langle 100 \rangle$. Instead leading order terms, such as $\Sigma_{\vec{k}}(k_x^4k_y^2+k_y^4k_z^2+k_z^4k_x^2)\vec{m}_{\vec{k}}\vec{m}_{-\vec{k}}$, align the skyrmion lattice along one of the $\langle 100 \rangle$ directions depending on the sign of its prefactor. Such an alignment is indeed observed in our study. The presence of the two domain populations thereby remains, however, surprising. It may either suggest that the disorder induces random prefactors of the relevant anisotropy term or that one of the domain populations is metastable.

A major remaining puzzle concerns the intensity distribution of the ZFC state, which is reminiscent of the partial order in MnSi.[23] Several scenarios[28–31] have been suggested with a nontrivial topology to explain the partial order in MnSi: for example, a metastable body centered multi-Q state[28] or weakly stratified skyrmion lines.[29] Thus the ZFC state and its metastable nature may hint at an abundance of randomly positioned topological defects.

In conclusion, our study of $Fe_{1-x}Co_xSi$ identifies a second material after MnSi in which a skyrmion lattice forms. In the ZFC state this system unexpectedly exhibits also metastable partial magnetic order possibly related to spin textures with nontrivial topology, a liquid of defects or a complex spin texture. As the skyrmion lattice in $Fe_{1-x}Co_xSi$ appears in a strongly doped semiconductor our study establishes skyrmion lattices as a general ordering phenomenon in magnetic materials.

We wish to thank A. Bauer, B. Binz, F. Birkelbach, S. Dunsiger, M. Garst, S. Legl, M. Kartsovnik, R. Ritz, R. Schwikowski, B. Russ, M. Vojta, J. Zweck, and W. Zwerger. Financial support through Grant No. SFB608 of the DFG and NSF grant PHY05-51164 is gratefully acknowledged.

*Christian.Pfleiderer@frm2.tum.de

[1] S. Mühlbauer, B. Binz, F. Jonietz, C. Pfleiderer, A. Rosch, A. Neubauer, R. Georgii, and P. Böni, Science **323**, 915 (2009).
[2] A. Neubauer, C. Pfleiderer, B. Binz, A. Rosch, R. Ritz, P. G. Niklowitz, and P. Böni, Phys. Rev. Lett. **102**, 186602 (2009).
[3] A. N. Bogdanov and D. A. Yablonskii, Sov. Phys. JETP **68**, 101 (1989).
[4] T. H. R. Skyrme, Nucl. Phys. **31**, 556 (1962).
[5] I. Klebanov, Nucl. Phys. B **262**, 133 (1985).
[6] S. L. Sondhi, A. Karlhede, S. A. Kivelson, and E. H. Rezayi, Phys. Rev. B **47**, 16419 (1993).
[7] L. Brey, H. A. Fertig, R. Cote, and A. H. MacDonald, Phys. Rev. Lett. **75**, 2562 (1995).
[8] A. N. Bogdanov, U. K. Rößler, and A. A. Shestakov, Phys. Rev. E **67**, 016602 (2003).
[9] G. Aeppli and Z. Fisk, Comments Condens. Matter Phys. **16**, 155 (1992).
[10] D. Shinoda and S. Asanabe, J. Phys. Soc. Jpn. **21**, 555 (1966).
[11] J. Beille, J. Voiron, and M. Roth, Solid State Commun. **47**, 399 (1983).
[12] N. Manyala, Y. Sidis, J. DiTusa, G. Aeppli, D. Young, and Z. Fisk, Nature (London) **404**, 581 (2000).
[13] Y. Onose, N. Takeshita, C. Terakura, H. Takagi, and Y. Tokura, Phys. Rev. B **72**, 224431 (2005).
[14] J. Beille, J. Voiron, F. Towfiq, M. Roth, and Z. Y. Zhang, J. Phys. F: Met. Phys. **11**, 2153 (1981).
[15] S. V. Grigoriev, S. V. Maleyev, V. A. Dyadkin, D. Menzel, J. Schoenes, and H. Eckerlebe, Phys. Rev. B **76**, 092407 (2007).
[16] S. V. Grigoriev, D. Chernyshov, V. A. Dyadkin, V. Dmitriev, S. V. Maleyev, E. V. Moskvin, D. Menzel, J. Schoenes, and H. Eckerlebe, Phys. Rev. Lett. **102**, 037204 (2009).
[17] K. Ishimoto, Y. Yamaguchi, J. Suzuki, M. Arai, M. Furusaka, and Y. Endoh, Physica B **213-214**, 381 (1995).
[18] M. Takeda, Y. Endoh, K. Kakurai, Y. Onose, J. Suzuki, and Y. Tokura, J. Phys. Soc. Jpn. **78**, 093704 (2009).
[19] M. Uchida, Y. Onose, Y. Matsui, and Y. Tokura, Science **311**, 359 (2006).
[20] P. Bak and M. H. Jensen, J. Phys. C **13**, L881 (1980).
[21] O. Nakanishi, A. Yanase, A. Hasegawa, and M. Kataoka, Solid State Commun. **35**, 995 (1980).
[22] M. Tanaka, H. Takayoshi, M. Ishikawa, and Y. Endoh, J. Phys. Soc. Jpn. **54**, 2970 (1985).
[23] C. Pfleiderer, D. Reznik, L. Pintschovius, H. v. Löhneysen, M. Garst, and A. Rosch, Nature (London) **427**, 227 (2004).
[24] K. Shimizu, H. Maruyama, H. Yamazaki, and H. Watanabe, J. Phys. Soc. Jpn. **59**, 305 (1990).
[25] To obtain the data shown in Figs. 1(A)–1(C) the sample was rotated with respect to the vertical axis by fixed angles. The intensity maxima for $\langle 110 \rangle$ are the only way to explain the intensity patterns shown in Figs. 1(A)–1(C) consistently. This confirms the sample orientation independently.
[26] For $x=0.25$ the intensity of the maxima for the various $\langle 110 \rangle$ directions is not exactly identical.
[27] S. Mühlbauer, C. Pfleiderer, P. Böni, M. Laver, E. M. Forgan, D. Fort, U. Keiderling, and G. Behr, Phys. Rev. Lett. **102**, 136408 (2009).
[28] B. Binz, A. Vishwanath, and V. Aji, Phys. Rev. Lett. **96**, 207202 (2006).
[29] U. K. Rößler, A. N. Bogdanov, and C. Pfleiderer, Nature (London) **442**, 797 (2006).
[30] S. Tewari, D. Belitz, and T. R. Kirkpatrick, Phys. Rev. Lett. **96**, 047207 (2006).
[31] I. Fischer, N. Shah, and A. Rosch, Phys. Rev. B **77**, 024415 (2008).